



Design of nanoporous interfacial SiO₂ layer in polysiloxane-graphene oxide nanocomposites for efficient stress transmission

Journal:	<i>RSC Advances</i>
Manuscript ID	RA-ART-04-2016-010745.R1
Article Type:	Paper
Date Submitted by the Author:	30-May-2016
Complete List of Authors:	Wang, Hualan; Hangzhou normal University, Wu, Jirong; Hangzhou Normal University, Gong, Kai; School of Pharmaceutical Science, Jiangnan University, Hao, Qingli; Nanjing University of Science and Technology Wang, Xin; Nanjing University of Science and Technology Jiang, Jianxiong; Hangzhou Normal University, Key Laboratory of Organosilicon Chemistry and Material Technology Li, Zhifang; Hangzhou Normal University Lai, Guoqiao; Hangzhou Normal University
Subject area & keyword:	Composites < Materials



Journal Name

ARTICLE

Design of nanoporous interfacial SiO₂ layer in polysiloxane-graphene oxide nanocomposites for efficient stress transmission

Hualan Wang,^{a,*} Jirong Wu,^{a,*} Kai Gong,^b Qingli Hao,^c Xin Wang,^c Jianxiong Jiang,^{a,*} Zhifang Li,^a and Guoqiao Lai^a

Received 00th January 20xx,
Accepted 00th January 20xx

DOI: 10.1039/x0xx00000x

www.rsc.org/

Interfacial interaction between graphene oxide (GEO) sheets and polysiloxane is important for the applications of GEO based silicone systems. However, polysiloxane is one of the polymers suffering from poor affinity with graphene oxide, which has become a bottleneck for the integration and applications of GEO in such polymer matrixes. Here we introduce an effective approach to solve the problem by employing SiO₂ as interfacial layers. Being compatible with both GEO and silicone, the interfacial layer is nanoporous and tunable. Firstly, GEO was modified with nanoporous SiO₂ via a sol-gel process. Secondly, GEO/SiO₂ (GEOS) was integrated into fluid-like hydroxyl terminated polydimethylsiloxane (PDMS-OH) through a solvent-free blending process. Thirdly, GEOS/PDMS-OH matrix was vulcanized at room temperature (RTV), forming the final silicon rubber (SR) elastomer. A tensile strength of 3.36 MPa and a Young's modulus of 3.38 MPa were achieved for RTV SR elastomer, higher than those of GEO (0.69 and 1.40 MPa) and fumed SiO₂ (1.32 and 2.2 MPa) based ones at the same filling fractions, respectively. The strong interactions between SiO₂ and GEO, as well as excellent compatibility between SiO₂ and PDMS-OH, have made SiO₂ act as a bridge of stress transmission between GEO and PDMS-OH. Simultaneously, the adjustable nanoporous architecture at the GEO/PDMS-OH interface was demonstrated to be an important contributing factor for enhanced stress transmission and mechanical properties.

1. Introduction

Functional polymers have attracted considerable academic and industrial interests due to their remarkable electrical, thermal, mechanical performances and promising applications.^{1–3} Polymers usually show special properties with the addition of particles with micron or macro dimensions,^{4–7} including our previous work on the synthesis of graphene based conducting polymer energy storage materials.^{8–11} Particle dispersion is a prerequisite,^{12,13} which is hard for certain particles due to the lack of thermodynamic compatibility with polymer matrixes, making further applications difficult. A number of strategies have been reported to improve the interface interactions and dispersion of polymer nanocomposites.^{14–19}

Polysiloxane,²⁰ or silicone, is one of such polymers which requires the aid of compatible fillers to achieve special properties in many cases. Polysiloxane has received extensive attention for

advantageous physical properties brought by siloxanes, whose backbone consist highly flexible repeated hydrophobic Si—O—Si bonds. The unique physical properties of silicone include: good permeability, very low glass-transition temperature (T_g), low surface energy, good UV resistance and optical clarity.²¹ These excellent performances have prompted silicone to become an ideal candidate for high performance adhesives,²² elastomers,^{23, 24} protective coatings,²⁵ water repellents, biocompatible materials,²⁶ plasticizers²⁷ and so on.

Over the past few years inorganic fillers with multiple scales for polysiloxane were systematically studied, including layered silicates,²⁸ metal oxides,²⁹ carbon material,^{30, 31} metallic nanoparticles, mesoporous silicas,³² and layered double hydroxide,³³ to name a few. However, the integration of these nanofillers into polysiloxane often suffers from one or more shortcomings such as complicated mixing process using toxic organic solvents, lack of compatibility, short of uniform dispersion, low structural stability, short shelf life, unstable interfaces and imperfect performances. Therefore, developments of novel nanofillers and highly uniformly filled polysiloxane matrixes have been under permanent attention.

Graphene oxide (GEO),³⁴ the derivative of graphene, has a great potential for developing high performance polysiloxane and other polymer nanocomposites due to adjustable structure and fascinating properties of elasticity, stiffness, prestress^{35–38} and so on. However, the compatibility of GEO with polysiloxane is still an unwell solved problem which has limited the depth application of GEO. Some researchers proved that optimizing processing

^a Key Laboratory of Organosilicon Chemistry and Material Technology, Ministry of Education, Hangzhou Normal University, No.58, Haishu Rd, Hangzhou, 311121, China.

^b School of Pharmaceutical Science, Jiangnan University, No.1800, Lihu Avenue, Wuxi, 214122, China.

^c Key Laboratory of Soft Chemistry and Functional Materials, Ministry of Education, Nanjing University of Science and Technology, No.200, Xiao Lingwei Street, Nanjing, 210094, China.

* Corresponding authors. Email: hualanwang@163.com (Hualan Wang), 23wjw@163.com (Jirong Wu), fgeorge@21cn.com (Jianxiong Jiang).

Electronic Supplementary Information (ESI) available: [details of any supplementary information available should be included here]. See DOI: 10.1039/x0xx00000x

technique could help to improve the filler dispersion in epoxy matrix.³⁹ Other researchers believed that covalent functionalization of GEO was crucial to fabricate highly compatible and well dispersed polysiloxane matrixes, and to give new features.⁴⁰⁻⁴² Among these strategies, optimizing processing technique is simple and direct, the effect is strongly dependent on the compatibility between different components. Moreover, the effects of processing technique on dispersion in macro-scale and micro-scale are different, and the latter is much more difficult. Covalent functionalization of GEO is beneficial for the interfacial contacts between GEO and silicone, however, sometimes the use of toxic organic solvents is inevitable in the covalent modification process of GEO.⁴³ So far neither optimizing processing technique nor covalent functionalization has been demonstrated to be a universal solution, especially for the consideration of further improving dispersions, simplifying mixing procedures without toxic solvents, and scale industrial applications. Therefore, integration of GEO into silicone homogeneously is still a big challenge. Efforts to develop novel strategies to construct compatible and stable interfaces between GEO and polysiloxane with improved performances are becoming more and more important.

It is well known that the abundant oxygen-containing functional groups on GEO⁴⁴ have brought the possibility to form modified compounds with other nanoparticles or molecules.^{45, 46} If the modified nanoparticles are compatible with polysiloxane molecules, it will be possible to construct highly compatible and dispersed functional polysiloxane nanocomposites with improved performances.

Herein, we report an effective approach to achieve ideal dispersion of GEO in hydroxyl terminated polydimethylsiloxane (PDMS-OH) through a proper interface design using nanoporous SiO₂ as a compatible layer. We expect to observe extraordinary mechanical properties of prepared polymer matrix, and to understand the interfacial interactions and stress transfer processes between such non-covalent functionalized GEO and PDMS-OH.

2. Experimental section

2.1 Fabrication of graphite oxide (GO) and GEOS.

GO was prepared using graphite (500 mesh) according to other literature by Hummers method.⁴⁷ For preparation of GEOS, first, GO (5 g) was dispersed in ethanol/distilled water (DI-water) mixed solvents (5000 mL) with the volume ratios in the range from 1:10 to 10:1. The solution was ultrasonicated for 1 h in a KQ-600 ultrasonic cleaner (600 W, Kunshan Ultrasonic Instrument Co., Ltd., China) to form a partially peeled GEO dispersion. Here, Ultrasound has a strong exfoliation effect for GEO, despite that the high collision opportunities among GEO layers led to partly restacking. Second, tetraethylorthosilicate (TEOS, 186 mL) was slowly added into the GEO dispersion in succession in a flask (10000 mL) to stable and peel GEO in depth under ultrasound. Third, ammonium hydroxide (50 mL) was added into the mixture under slow stirring in the reaction vessel equipped with an electric stirring apparatus. Finally the stirring was terminated after reacting for 1 h. The product was collected by high speed

centrifugation at 10000 rpm for 10 min, then rinsing with distilled-water. The as-prepared product was dried in a vacuum oven at 80 °C overnight and left 55 g in weight, and the product was signed as GEOS. Based on this process, several analogous GEOS samples were also prepared by changing the relative amounts of raw materials. As for comparison, individual SiO₂ was prepared without GEO under the same conditions.

2.2 Blending processes of the GEOS/PDMS-OH mixtures.

PDMS-OH (hydroxyl terminated polydimethylsiloxane) with different viscosities ranging from 5000 to 500000 cP (Mw: 49300~300000) were used as polysiloxane substrates. Firstly, GEOS was grinded until all the powder can pass through a 100-mesh sieve. Secondly, GEOS (30 g) was premixed with PDMS-OH (100 g) by a MXD-F Lab dispersing stirring sand multi-purpose machine (Shanghai Mu Xuan Industrial Co., Ltd., China) for 60 min. After that, the mixture was collected and transferred to a SGM 65-II three-roll machine (Funing County chemical plant, China) with further mixing by the shear action between rollers for five times.

2.3 Vulcanization of the GEOS/PDMS-OH matrix

The well mixed GEOS/PDMS-OH mixture in section 2.2, TEOS, dibutyltindiacetate and 3-aminopropyltriethoxysilane (NH₂CH₂CH₂CH₂Si(OC₂H₅)₃, KH550) were mixed with the mass ratio 100:4:2:2. Here, TEOS, dibutyltindiacetate and KH550 serve as crosslinking agent, catalyst and silane coupling agent, respectively. After rapid mixing, the mixture was poured into a 12 ×12×0.25 cm square mold, which was previously covered with a polyimide film (thickness: 0.01 cm) on the mold bottom. The mixture was left natural leveling and solidifying at room temperature in air overnight, giving PDMS-OH elastomer. The piece was then cut into strips for mechanical tests.

2.4 Material characterization.

Morphological analyses of samples were carried out on an H-7650 transmission electron microscope (TEM, Hitachi, Japan) and an SEMS-3000N scanning electron microscope (SEM, Hitachi, Japan). Field emission scanning electron microscopy images were recorded on an S-4800 field emission scanning electron microscope (FE-SEM, Hitachi, Japan). N₂ isotherm results were obtained on an Autosorb-1 automatic physical and chemical adsorption analyzer (Quantachrome Instruments, USA). TGA data were recorded on a TG209C thermogravimetric analyzer (Netzsch, Germany) using a Al₂O₃ crucible in N₂ atmosphere at the speed 10 °C/min. Mechanical properties were recorded on a material testing machine (Gotech Testing Machines Co. LTD, China).

3. Result and discussion

3.1 Microcosmic character of GEOS

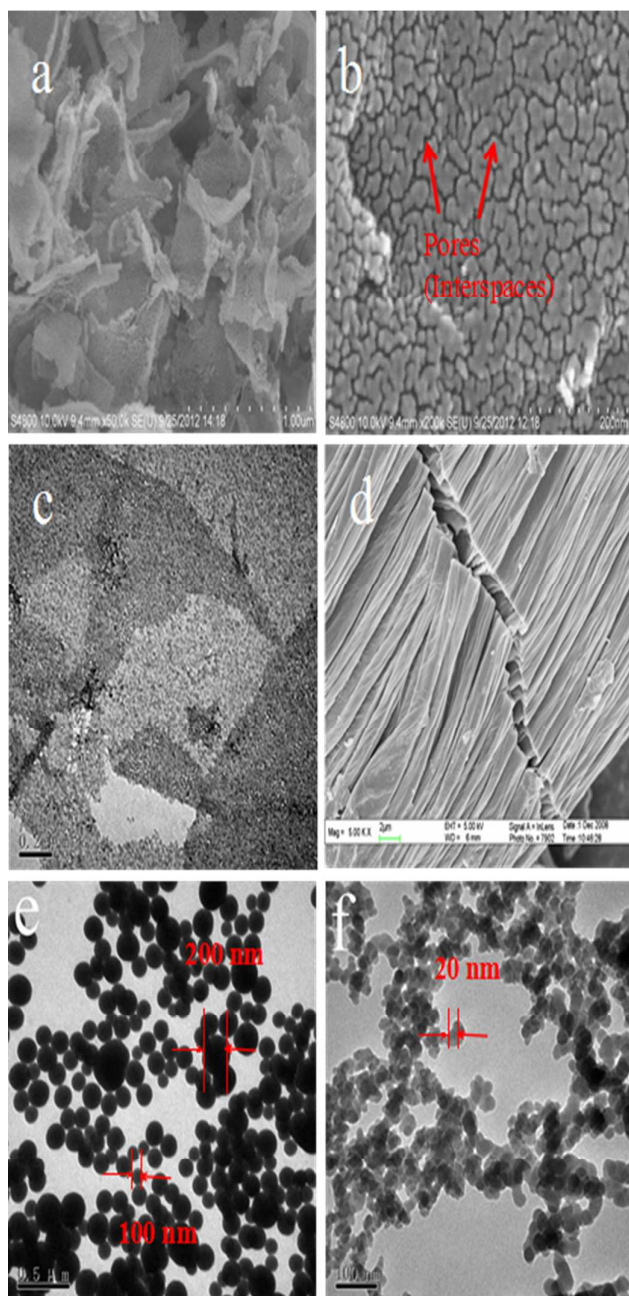


Figure 1. Figure 1 FE-SEM (a, b) and TEM (c) of GEOS, FE-SEM image (d) of GEO, TEM images of SiO₂ particles prepared without GEO (e) and fumed SiO₂ (f).

FE-SEM and TEM images of GEOS are shown in Figure 1(a, b) and Figure 1(c), respectively. GEOS is composed of different layers of approximately two-dimensional GEO covered with nanostructured SiO₂ on both sides. The sheet boundaries are clearly visible (Figure 1(a)), and from these boundaries a thickness of 20~40 nm is estimated for GEOS sheets. The SiO₂ size ranges from 10 to 20 nm, about half of the GEOS sheet thickness, indicating that GEO almost exists as mono-layers in GEOS. These mono-layers are obviously different with unmodified GEO sheets, which are in restacked state just as

shown in Figure 1(d). High magnification observations of GEOS (Figure 1(b)) reveal that irregular shaped amorphous SiO₂ nanoparticles tightly grow on GEO sheet surfaces and assemble into an open porous structure with narrow and long passages. The pores are only 10~20 nm in width, which is in the mesoporous range. These channel-shaped pores, universal and interconnected, are mainly driven by various interactions including hydrogen bonding and van der Waals attractions between SiO₂ and GEO as well as neighboring SiO₂ nanoparticles. For comparison, the TEM images of two kinds of individual SiO₂ are also recorded and shown in Figure 1(e, f). It is noteworthy that the particle size of SiO₂ (10~20 nm) in GEOS is much smaller than that of SiO₂ prepared without GEO (Figure 1(e)), around 80~200 nm, and also smaller than that of commercial fumed SiO₂ (Figure 1(f)) with the size 20~30 nm. GEO plays an important role in reducing the SiO₂ size, perhaps the existence of steric hindrance greatly prevents the growth of SiO₂ into larger size. On one hand, the densely and widely distributed oxygen-containing active positions on GEO have provided larger quantity of nucleation sites for growth of SiO₂ compared with the situation without GEO. On the other hand, both the growth and agglomeration tendency of SiO₂ are greatly inhibited by the existence of GEO sheets. Thus the size of SiO₂ tends to decrease in presence of GEO compared with the situation without GEO when the total amount of SiO₂ keeps constant. These are the main steric effects which restrict the size of SiO₂ nanoparticles to bigger size.

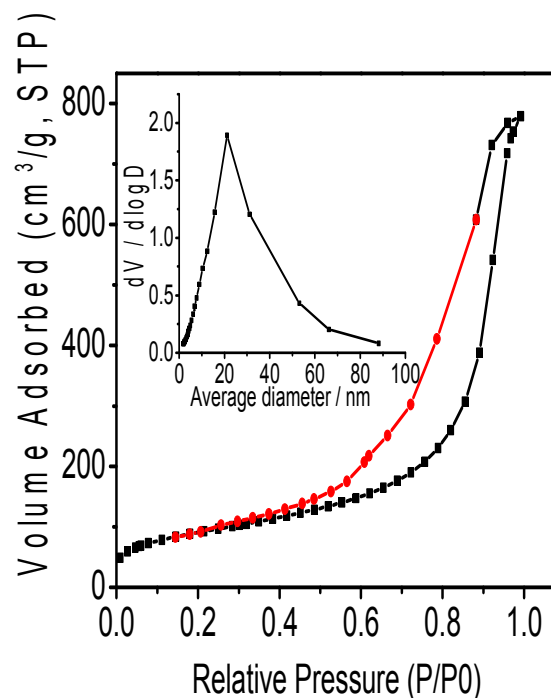


Figure 2. The N₂ isotherms plot of GEOS. The inset shows the pore size distribution of GEOS from BJH method. GEOS were prepared in ethanol/water mixture with the volume ratio 1:10.

N₂ isotherm is an effective method to determine whether a

sample owns porous structure and the details of pores. From the result of GEOS in Figure 2, we deduce that the N_2 isotherms is attributed to Type IV, which is characteristic of mesoporous materials.⁴⁸ The remarkable hysteresis loop over the range of $0.2 < P/P_0 < 1.0$ is further indicative of mesoporous architecture in GEOS. The pore size distributes in the range from 10 to 50 nm using the Barrett-Joyner-Halenda (BJH) method, and the most probable aperture of GEOS is close to 20 nm, as shown in the illustration of Figure 2. The high consistency of pore size recorded by FE-SEM and N_2 isotherm instruments indicates good uniformity of prepared GEOS sample. The Brunauer-Emmett-Teller (BET) surface area value reaches $545 \text{ m}^2 \text{ g}^{-1}$ based on the method in the literature.⁴⁹ This value is much higher than that of individual SiO_2 prepared without the addition of GEO ($\sim 20 \text{ m}^2 \text{ g}^{-1}$), and higher than that of commercial fumed SiO_2 about $100 \sim 380 \text{ m}^2 \text{ g}^{-1}$. The nanoporous architecture at the GEO surface is also expected to improve the mechanical properties of target polymer matrix.

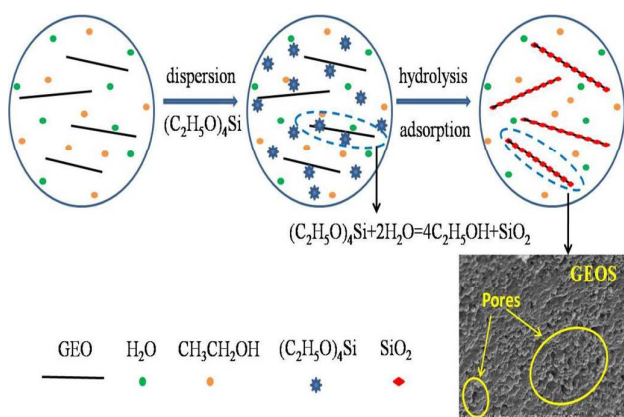
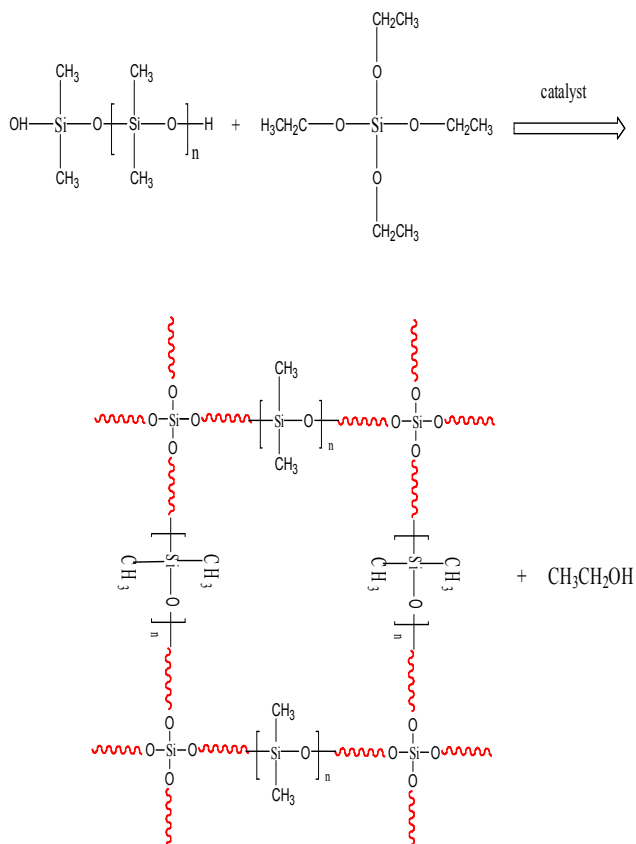


Figure 3. Proposed formation mechanism of nanoporous GEOS.

According to the above FE-SEM morphology, N_2 isotherm results, and TEM analysis, we suggest that the formation of the GEOS porous structure experienced an adsorption procedure first, followed by hydrolysis and assembling processes subsequently, just as shown in Figure 3. After TEOS was added into the GEO dispersion of ethanol/water mixed solvents under stirring, the silicon precursor molecules gradually adsorbed to the sheet surfaces driven by hydrogen bond and electrostatic interactions. When ammonia was added into the mixture, TEOS molecules on GEO surfaces gradually hydrolyzed and generated primary particles of SiO_2 in situ. Meanwhile, TEOS molecules in solvents also hydrolyzed and the generated SiO_2 particles moved to and self-assembled with the SiO_2 on GEO surfaces, forming clearance holes or growing into larger nanoparticles. The fast hydrolysis of TEOS enabled quick and facile modification within minutes at room temperature. The pores do not come from silica and GEO themselves, but from the gap between SiO_2 particles on GEO sheets and among different SiO_2 nanoparticles.

3.2 Enhancement models of SiO_2 , GEO and GEOS based PDMS-OH nanocomposites

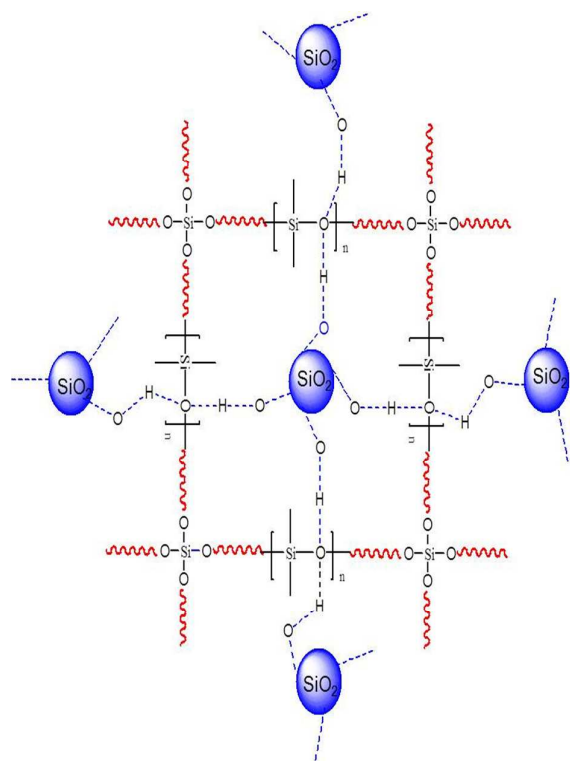
Many unfilled silicone networks display extremely poor mechanical properties, filled systems are stiffer, stronger, and tougher than their unfilled counterparts. In order to understand the enhancing mechanism of GEOS, it is necessary to point out the reinforcement principle of unfilled and filled PDMS-OH by individual SiO_2 and GEO. The reinforcing and stress transmission of unfilled PDMS-OH is realized mainly through cross-linking agents, as shown in Scheme 1. The cross-linking positions focus on the ends of each polymer molecule chain. Such a single action mode is clearly insufficient to obtain good mechanical strength. Suitable reinforcing filler should be added to generate strong crosslinked network structure, which may help to promote the stress transmission and improve the mechanical properties of such kind of non-self-reinforced polysiloxane molecules.



Scheme 1. The catalytic crosslinking process of PDMS-OH without fillers.

3.2.1 Point enhancement model of SiO_2 based PDMS-OH nanocomposites. When fumed SiO_2 is chosen as filler for PDMS-OH, the interactions among PDMS-OH molecular chains are no longer limited by cross-linking agents. Another strong link is achieved by lots of SiO_2 nanoparticles, just as shown in Scheme 2. The chain of PDMS-OH is constituted by the repeated units of $-\text{Si}-\text{O}-$, which has excellent compatibility with SiO_2 . Sufficient and stable contacts can be realized at the SiO_2 /PDMS-OH interfaces through hydrogen bond. SiO_2 nanoparticles, each with a number of PDMS-OH molecules

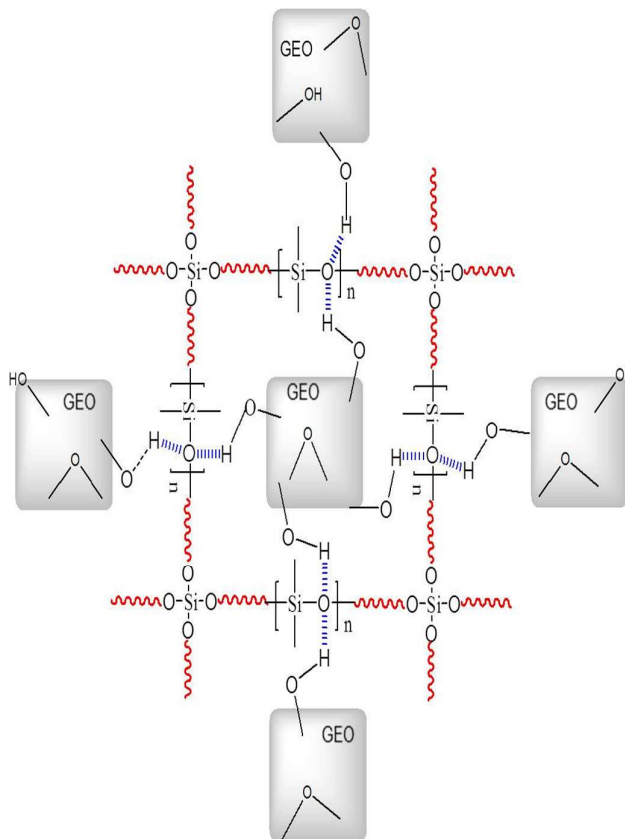
around, behave like big strong hands, firmly grasp the surrounding PDMS-OH molecule chains when external force is applied to the sample. Here stress shifts from polymers to SiO_2 nanoparticles, then to the adjacent polymers, thus extending down so as to digest external force. Therefore, SiO_2 endows PDMS-OH enhanced mechanical strength through such kind of interfacial stress transfer^{50, 51}.



Scheme 2. The point enhancement model of SiO_2 in PDMS-OH nanocomposites.

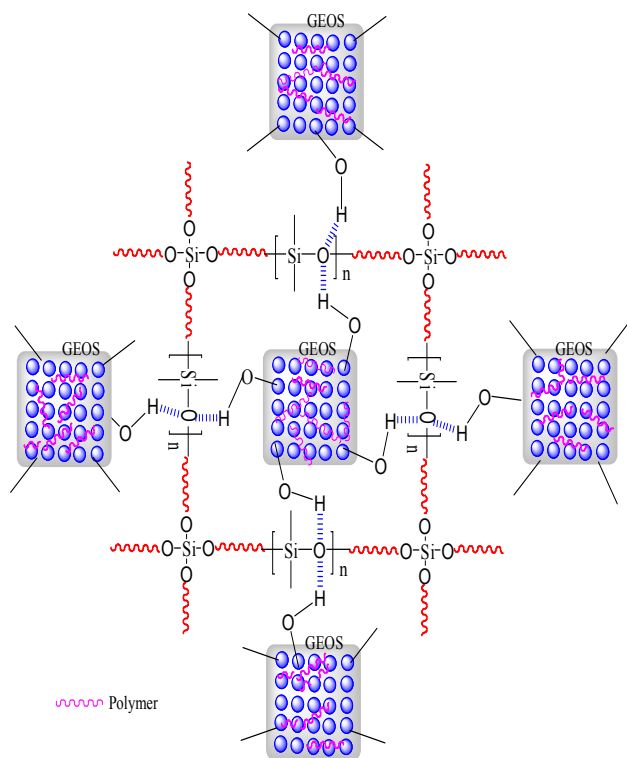
3.2.2 Plane enhancement model of GEO based PDMS-OH nanocomposites. When individual GEO is integrated into PDMS-OH, stress transmission occurs at GEO surface in the form of a plane enhancement model, just as shown in scheme 3. Abundant hydrogen bonds between GEO and PDMS-OH combined with chemical crosslinking among PDMS-OH molecules have dominated the interactions. Theoretically, compared with point enhancement model, plane enhancement model should provide stronger interactions among different PDMS-OH chains due to more contact opportunities between GEO and PDMS-OH. However, the compatibility of GEO is not as good as SiO_2 with PDMS-OH, leading to the reunion tendency of GEO. Therefore GEO encounters inadequate interface contacts and unsatisfactory dispersion in PDMS-OH, which perhaps reduces stress transfer effect at the interfaces. Luckily, we are inspired from the phenomenon and results of SiO_2 filled PDMS-OH matrixes. Since good compatibility and adequate interfacial contacts are essential and have been realized for the stress transmission

between SiO_2 and PDMS-OH, how about trying the modification of GEO with SiO_2 ? So we designed and fabricated the nanoporous GEO surfaces by introduction of SiO_2 just as mentioned in the former texts.



Scheme 3. The plane enhancement model of GEO in PDMS-OH nanocomposites.

3.2.3 Point & plane enhancement model of GEOS based PDMS-OH nanocomposites. The junctions are, in addition to crosslinking agent molecules, mainly irregular SiO_2 nanoparticles and 2D GEO nanosheets for SiO_2 and GEO based matrixes, respectively. The GEOS filled PDMS-OH composites, however, have created a more powerful 3D network conjunctions constituted by SiO_2 nanoparticles, 2D GEO nanosheets, crosslinking agent molecules and physical connection simultaneously, a total of four kinds of conjunctions, just as shown in Scheme 4. The advantages of point & plane enhancement model include the nanosize, high aspect ratio, affinity of GEOS, and the nanoporous architecture of SiO_2 between GEO and the host polymer matrix. The interfacial layer SiO_2 is verified to have strong interactions with GEO (see supplementary Figure S1, FTIR) and PDMS-OH, which is a basis for stress transfer between GEO and PDMS-OH. Driven by macro- and nano- scale filler junctions, the point & plane model is expected to exhibit better stress transfer and show synergy in improving the mechanical properties of GEOS based PDMS-OH nanocomposites.



Scheme 4. The point & plane enhancement model of GEOS in PDMS-OH nanocomposites.

3.3 Mechanical performances and experimental validations

The tensile strength of additive-free cross-linked PDMS-OH (5000 cP) is only 0.2 MPa, while the values for GEOS, fumed SiO_2 , GEO, and SiO_2 fabricated without GEO based PDMS-OH nanocomposites increase to 1, 0.7, 0.5 and 0.26 MPa respectively when 10 wt.% of fillers are added. And the values further increase to 1.8, 1.32, 0.7, and 0.51 MPa, respectively when filler content increases to 30 wt.%, just as shown in Figure 4. These fillers can be sorted according to the enhancing effect as following: GEOS > fumed SiO_2 > GEO > SiO_2 prepared without GEO. Also, the tensile strength of PDMS-OH matrixes can be conveniently adjusted by changing the filling fractions of GEOS. Being benefit from stronger interfacial interactions, GEOS exhibits the leading enhancing among all these fillers. GEOS based matrix reaches 9 times compared with the additive-free one, and more than two times compared with the GEO filled one. According to the raw material and product weights, the mass ratio of GEO and SiO_2 in GEOS is estimated to be 1:10. That is to say, the content of GEO in polymer matrix is about 3 wt. %.

Note that there is a common feature for all these fillers: The tensile strength value keeps increasing as the filler fraction raises (especially >10 wt.%) until achieving the upper threshold 30 wt.%, after which there is a downward trend. Perhaps the phenomenon could be explained as follows. When the filler content is very little, the dispersion of filler particles in the polymer matrix has not formed the network structure, the role of the particles is relatively weak, and the promotion on mechanical properties is also limited. With the increase of the

filling fraction (>10 wt. %), particles gradually form interconnected network structure and play an increasingly significant role of promoting the polymer properties. In the process, the sample performance experiences a gradually accumulating course. However, a performance decrease emerges after 30 wt. % of the filler fraction. On one hand, the hydrogen bonds between GEOS surfaces and PDMS-OH molecules gradually intensify as the filler content increases. As a result, the GEOS/PDMS-OH system becomes more and more viscous and the mobility of the system gradually decreases, namely thickening phenomenon. On the other hand, excess fillers occupy a great amount of physical space, partly blocking the channel of polymer inter-molecular cross-linking, leading to insufficient vulcanization. So, over high dosage deteriorates the mechanical performances.

In terms of GEOS based PDMS-OH matrix, SiO_2 not only reduces the stacking tendency of GEO, but also promotes the specific area utilization efficiency of GEO, and further greatly promotes the compatibility between GEO and PDMS-OH substrates (see supplementary Figure S2, XRD). Therefore, the dispersion of GEOS in PDMS-OH is comparable to that of SiO_2 , and better than that of GEO. When integrated into the polymer matrix in the form of GEOS, GEO have separated from the original stacks and dispersed in individual or very thin layers instead of aggregating into agglomerates. Therefore, the point & plane enhancement model has aroused the advantages of both points and plane models, exhibiting greater enhancing effect. The detailed blending and forming procedures of the GEOS/PDMS-OH based nanocomposites was shown in supplementary Figure S3.

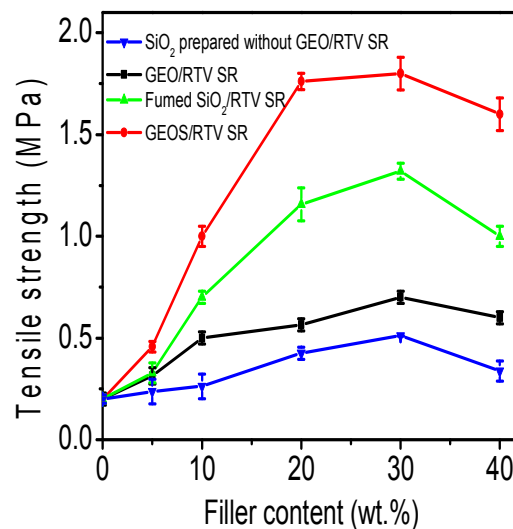


Figure 4. The tensile strength of PDMS-OH elastomers filled by GEOS, GEO, fumed SiO_2 and the SiO_2 prepared without GEO as a function of filler content.

Improvements of tensile strength results have verified the effect of point & plane enhancement model initially. The relationship between Young's modulus and filler content was also studied to further assess the performances of prepared RTV SR, just as shown in Figure 5. The tensile modulus values

of GEOS and fumed SiO_2 based RTV SR composites have the same trends as that of tensile strength. Unlike GEOS and SiO_2 , the modulus trends of RTV SR filled by GEO and self-prepared SiO_2 are a little different, which is related to the nature of fillers. However, it is clear that the modulus values have the same sequence as that of tensile strength: GEOS > fumed SiO_2 > GEO > SiO_2 prepared without GEO at the dosage 30 wt. %. And at this fraction point the modulus values are 2.43, 2.2, 1.4 and 1.05 MPa, respectively. The improvement of mechanical performances may be attributed to at least two factors. The first is the nanoporous architecture brought by the introduction of SiO_2 at GEO/PDMS-OH interfaces, the second is the improved dispersion (see supplementary Figure S4, SEM) due to better interfacial contacts and larger interactions. Conventional routes to reinforce polysiloxane are realized mostly by adding commercial fumed SiO_2 , which is prepared from SiCl_4 , CH_3SiCl_3 or SiF_4 under a temperature of more than 1000°C ⁵². Such a high temperature leads to high energy consumption and costs. Different from conventional method and covalent modification of GEO, our approach is a moderate, easy batch preparation, high efficient and non-destructive way, which maximumly retains the skeleton microstructure and mechanical properties of lamellar GEO. The solution is simple, both the filler preparation and composite blending processes can be completed at room temperature without toxic organic solvents, quite adapt to the requirements of green material chemistry and polymer nanocomposites.

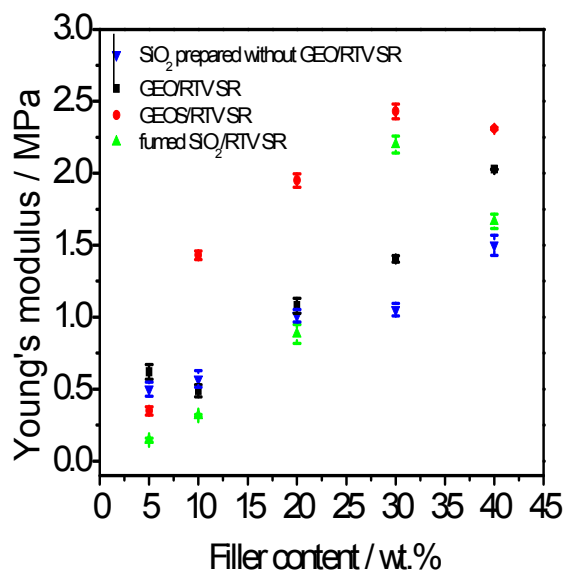


Figure 5. Young's modulus of the as-prepared PDMS-OH elastomer filled by GEOS, GEO, fumed SiO_2 and SiO_2 prepared without GEO.

A thermal gradient curing experiment is tried for the PDMS-OH matrixes filled by 30 wt.% of GEOS with the mass ratio 1:15. By changing the curing temperature from 20 to 35, 50 and

65°C , the tensile strength values of 1.60, 1.62, 1.66 and 2.48 MPa and the modulus values of 3.16, 3.32, 3.45 and 3.97 MPa are achieved, respectively. One can see that temperature is another influencing factor related to the mechanical properties. Generally, the temperature effect on tensile strength is not obvious, or only slight rise under 50°C . However, there is a significant tensile strength increase when the temperature achieves 60°C , showing a bigger improvement, just as shown in figure 6. Compared with tensile strength, modulus changes with the temperature more significantly, a bigger modulus response is seen below 50°C , which is also a turning point of performance. In addition to this, the thermal gradient curing experiment was also done in a different way. It was carried out by heating one side of the square sample to 65°C and keeping the other side in the room temperature environment. The sample was then cut into strips along the direction of temperature change for mechanical tests. The results show that there are no real distinctions among these different strips. One possible reason is that the sample itself has a certain thermal conductivity, which makes the temperatures at different locations in the sample tend to be consistent in the curing process.

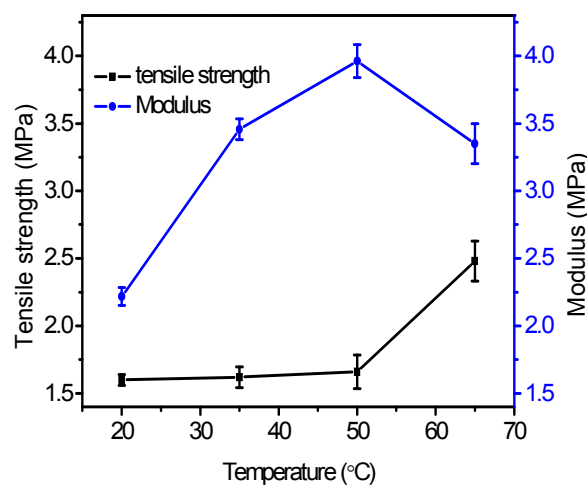


Figure 6. Tensile strength and modulus of the GEOS/PDMS-OH nanocomposites as a function of temperature. GEOS with the mass ratio 1:15 (GEO: SiO_2) here constitutes 30 wt.% of the PDMS-OH matrix.

The amount of GEO is small compared to the SiO_2 in GEOS (1:10 and 1:15) for the above results. Further discussion on GEOS/PDMS-OH nanocomposites is needed about the situation when changing the relative amount of GEO and SiO_2 in GEOS and mixed solvent ratio while keeping the viscosity of PDMS-OH constant (5000 cP). Therefore, GEOS with different mass ratios (GEO: SiO_2) are prepared in mixed solvents of ethanol and DI-water with the volume ratio of 10:1. Figure 7 summarizes the corresponding results showing the tensile strength and Young's modulus as a function of the mass ratio. As the mass ratio changes from 1:15 to 1:10, PDMS-OH matrixes show better mechanical performances. The peak values for tensile strength and Young's modulus are 2.0 and

2.65 MPa, respectively, corresponding to the mass ratio 1:10. Continuing increase of GEO in GEOS leads to a performance decrease. Despite this, the mechanical strength values of GEOS/PDMS-OH nanocomposites have risen in varying degrees compared to GEO/PDMS-OH and SiO₂/PDMS-OH nanocomposites in our experimental range. So the relative contents of GEO and SiO₂ in GEOS are important for the final mechanical performances of the corresponding polymer matrixes. And the point & plane enhancement model is still effective under changed mass ratios for GEOS based PDMS-OH nanocomposites.

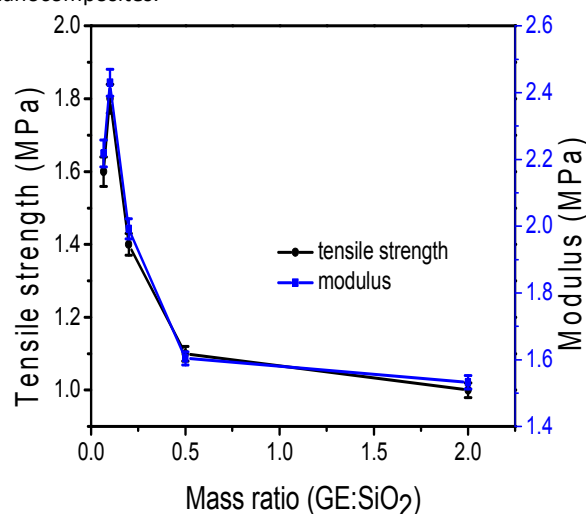


Figure 7. Tensile strength and modulus of the GEOS/PDMS-OH nanocomposites as a function of mass ratio (GEO: SiO₂) in GEOS at the filling fraction of 30 wt. %, GEOS were prepared in ethanol/water mixture with the volume ratio 10:1.

Inspired by the above results, we carried out experiments using GEOS (1:10) and PDMS-OH with different viscosities from 5.0X10³ to 5.0X10⁵ cP to further reveal the potential of GEOS on the mechanical properties of PDMS-OH based RTV silicon rubber. Figure 8 shows the tensile strength and modulus values of GEOS/PDMS-OH elastomers as a function of the PDMS-OH viscosity. The tensile strength rapidly increases with growing PDMS-OH viscosity in the range of 10³ -10⁵ cP, after which the value slowly increases. The tensile strength value rises from 1.8 MPa to 3.363 MPa within our experimental viscosity range, which is enough for PDMS-OH based RTV SR in many applications. For example, they can be used as sealants for power batteries and solar panels in civilian areas. They are also promising to act as adhesives for parts in aircraft or armor for defense. The good mechanical performances and elasticity of RTV SR can well adapt to the frequent vibrations, limit operating temperatures and complex environments of the military equipment. Meanwhile, the Young's modulus also changes with the PDMS-OH viscosity, and the highest value of 3.389 MPa emerges at 2.0X10⁴ cP, higher Young's modulus value means smaller elastic deformation under external force. Therefore, the lower Young's modulus value of 1.84 MPa at 1.0X10⁵ cP indicates relatively larger elastic deformation.

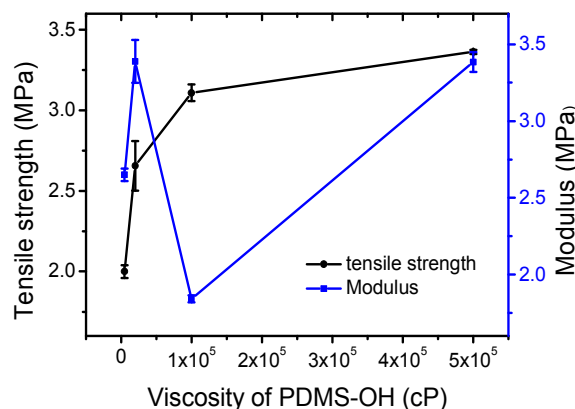


Figure 8. Tensile strength and modulus of GEOS/PDMS-OH matrixes as a function of PDMS-OH viscosity from 5.0 X 10³ to 5.0 X 10⁵ cP.

We also tested the tear strength values of RTV SR composites to see the transverse mechanical properties. Taking PDMS-OH with the viscosity of 5000 cP for example, a tear strength of 4.09 kN/m was achieved when filled with 30 wt.% of GEOS(1:10), higher than 1.62 kN/m for the GEO filled one. Higher value can be obtained when increasing the viscosity of PDMS-OH, just like the situation of tensile strength. And a tear strength value 10.43 kN/m was achieved for RTV SR elastomer when the viscosity of PDMS-OH increased to 5.0X10⁵ cP. Besides, the tear strength values for RTV SR composites were also tested when the PDMS-OH viscosity changes from 5.0X10³ to 5.0X10⁵ cP, just as shown in figure 9.

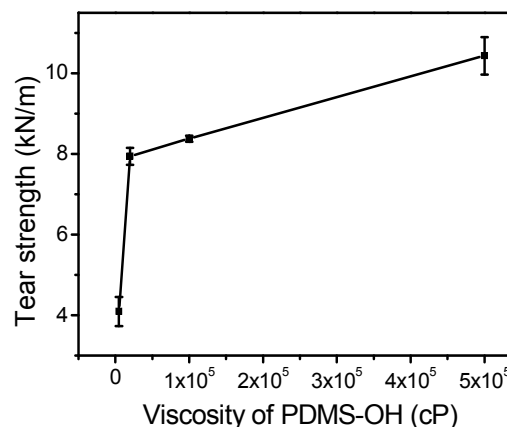


Figure 9. Tear strength of GEOS/PDMS-OH matrixes as a function of PDMS-OH viscosity from 5.0 X 10³ to 5.0 X 10⁵ cP.

It can not be ignored that there is a special inherent porous structure in GEOS, which is caused by the combination of approximate two-dimensional GEO and nanoscale SiO₂. These pores at the interfaces provide adequate anchoring spaces for tips of PDMS-OH chains through hydrogen bonds or clasping physically. This kind of anchoring, which is similar to the role of gear engagement, universal and powerful, can effectively help promote the stress transfer between PDMS-OH and GEOS. To understand the effect of the mass ratio of GEO and SiO₂ on the

mechanical performances of GEOS/PDMS-OH nanocomposites, N_2 adsorption isotherms of GEOS with different mass ratios are compared. Figure 10a-d show the corresponding results for the ratios 2:1, 1:5, 1:10, 1:15, respectively. From the Y-axis deflection curve with an inflection point at low pressure section, as well as the hysteresis loop at middle pressure segment, one can learn that all these N_2 adsorption isotherms are attributed to Type IV. Generally, larger P/P_0 for the occurrence of capillary condensation and bigger hysteresis loop mean larger aperture.

Figure 10e-h further show the BJH pore size distributions of GEOS for the ratios 2:1, 1:5, 1:10, 1:15, respectively. Taking the desorption branch for example, the most probable aperture of GEOS at the ratio 2:1 is 3.9 nm with a narrow peak, which is speculated coming from the stacked apertures between GEO sheets and SiO_2 granules that are directly contacted with GEO. Besides the peak of 3.9 nm, a new peak emerges in GEOS for the ratios 1:5, 1:10 and 1:15, situating at 29.5, 13.7 and 9.3 nm, respectively. The newly emerged peaks are all in the mesoporous range, and are possibly contributed by the apertures among the neighboring SiO_2 nanoparticles. This is possibly because that the particle contacts are no longer confined between GEO and SiO_2 when the quantity of SiO_2 increases to a certain extent. Instead, more contact opportunities among neighboring SiO_2 nanoparticles have

formed new stacking holes. Also, as the quantity of SiO_2 increases, the particle size of SiO_2 follows a downward trend, which leads to a size decrease tendency of the stacked apertures among SiO_2 , just as seen from the pore size distribution results. Meanwhile, there is a narrowing tendency for the newly appeared peak in figure 10e-h, indicating that the pore distribution of GEOS becomes more and more uniform. Perhaps it is one of the reasons that the mechanical performance tends to improve from 2:1 to 1:10, just as shown in figure 7. GEOS with the ratio 1:10 exhibits the maximum enhancement effect, indicating that its pore size and distribution are most suitable for improving the mechanical properties of PDMS-OH matrixes than other ratios. Continuing increase of SiO_2 in GEOS (1:15) leads to a performance decrease. Therefore, both the pore structures and the mechanical performances are adjustable in a certain range, and according to their relationships one can prepare desired nanocomposites.

Excellent interfacial interaction exists not only between SiO_2 and GEO, but also between SiO_2 and PDMS-OH. In a word, the property enhancements originate from the nanoporous architecture, improved compatibility, combination of advantages of point and plane enhancement models and the special interactions between GEOS and PDMS-OH molecules.

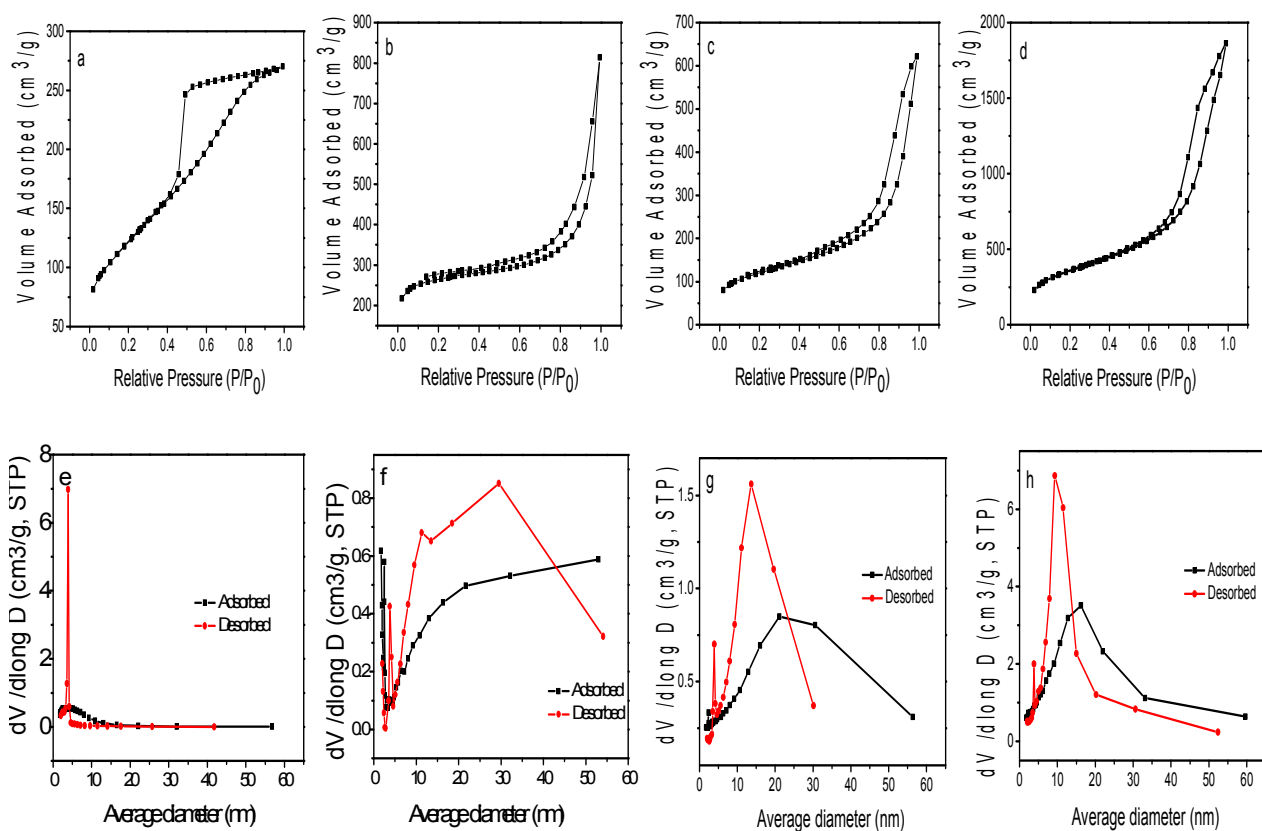


Figure 10. N_2 adsorption isotherms (77K) (a-d) and pore size distribution curves (e-h) of GEOS at different mass ratios (GE: SiO_2 = 2:1, 1:5, 1:10, 1:15). GEOS were prepared in ethanol/water mixture with the volume ratio 10:1.



Journal Name

ARTICLE

4. Conclusions

A high efficient approach was proposed to improve the stress transmission in GEO/PDMS-OH nanocomposites by the integration of adjustable nanoporous SiO₂ interfacial layer. Ultrahigh dispersed state of GEO in PDMS-OH was achieved, and the mechanical properties of GEOS based PDMS-OH elastomers were enhanced greatly through this strategy. The introduced SiO₂ not only increased the compatibility and interface contacts of GEO with PDMS-OH, but also served as a bridge of stress transfer between them. Point & plane enhancement model of GEOS based PDMS-OH elastomers has shown better mechanical performances and stress transfer effect than individual models. The enhancing mechanism is mainly attributed to the improved interfacial architecture and the strengthened interactions between GEO and PDMS-OH. This strategy provides an attractive low carbon path to large-scale synthesis of novel enhancing filler GEOS, which is foreseeable especially in but not limited to silicone industry. The method is also with great prospects in other occasions when it is necessary to improve the interfacial interactions or a solvent-free green blending process is in great demand, quite popular in both laboratories and industries.

Acknowledgements

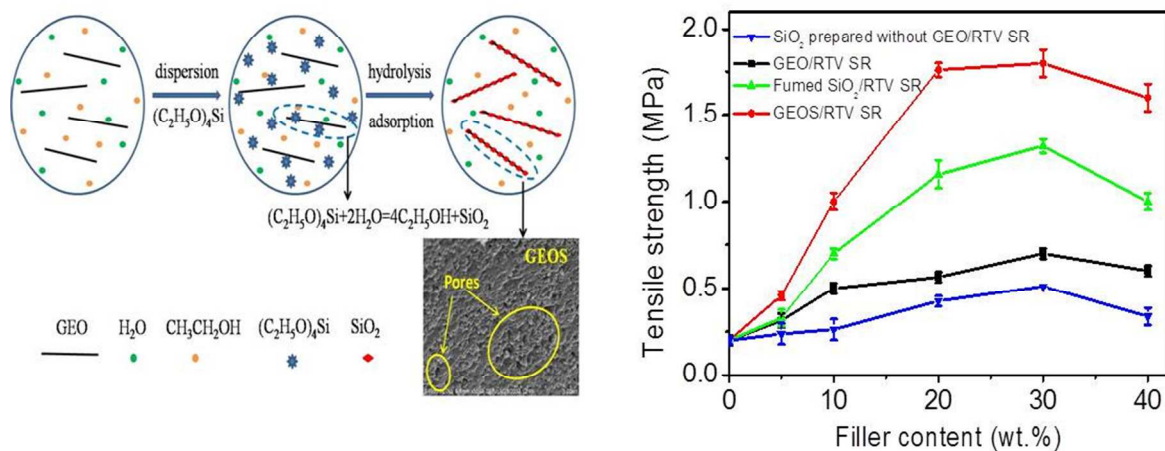
This work was supported by the National Natural Science Foundation of China (No.21303036, 51303069, 21576138 and 51572125), Zhejiang Provincial Natural Science Foundation of China (LQ13B040002), Start-up Fund of Hangzhou Normal University (2012QDL021), the Fundamental Research Funds for the Central Universities of China (No.30920130111003 and 30920140122003). Program for NCET-12-0629, the Ph. D. Programs Foundation of Ministry of Education of China (No.20133219110018), Qing Lan Project and Six Major Talent Summit (XNY-011), the Science and Technology Support Plan (No. BE2013126), and PAPD of Jiangsu Province, China.

References

1. C. Park, Y. La, T. H. An, H. Y. Jeong, S. Kang, S. H. Joo, H. Ahn, T. J. Shin and K. T. Kim, *Nat Commun*, 2015, **6**, 6392-6400.
2. S. H. Liu, P. Gordiichuk, Z. S. Wu, Z. Y. Liu, W. Wei, M. Wagner, N. Mohamed-Noriega, D. Q. Wu, Y. Y. Mai, A. Herrmann, K. Mullen and X. L. Feng, *Nat Commun*, 2015, **6**, 8817-8825.
3. Z. R. Wang, H. L. Dong, T. Li, R. Hviid, Y. Zou, Z. M. Wei, X. L. Fu, E. J. Wang, Y. G. Zhen, K. Norgaard, B. W. Laursen and W. P. Hu, *Nat Commun*, 2015, **6**, 7478-7488.
4. W. Dai, J. H. Yu, Z. D. Liu, Y. Wang, Y. Z. Song, J. L. Lyu, H. Bai, K. Nishimura and N. Jiang, *Compos Part a-Appl S*, 2015, **76**, 73-81.
5. L. B. Zhang, J. Q. Wang, H. G. Wang, Y. Xu, Z. F. Wang, Z. P. Li, Y. J. Mi and S. R. Yang, *Compos Part a-Appl S*, 2012, **43**, 1537-1545.
6. S. Grubjesic, B. S. Ringstrand, K. L. Jungjohann, S. M. Brombosz, S. Seifert and M. A. Firestone, *Nanoscale*, 2016, **8**, 2601-2612.
7. L. R. Liang, C. Y. Gao, G. M. Chen and C. Y. Guo, *J Mater Chem C*, 2016, **4**, 526-532.
8. H. L. Wang, Q. L. Hao, X. J. Yang, L. D. Lu and X. Wang, *Electrochem Commun*, 2009, **11**, 1158-1161.
9. H. L. Wang, Q. L. Hao, X. J. Yang, L. D. Lu and X. Wang, *Nanoscale*, 2010, **2**, 2164-2170.
10. H. L. Wang, Q. L. Hao, X. J. Yang, L. D. Lu and X. Wang, *Acs Appl Mater Inter*, 2010, **2**, 821-828.
11. Q. L. Hao, H. L. Wang, X. J. Yang, L. D. Lu and X. Wang, *Nano Res*, 2011, **4**, 323-333.
12. V. Khoshkava and M. R. Kamal, *Acs Appl Mater Inter*, 2014, **6**, 8146-8157.
13. Z. Su, H. Wang, F. Xu, K. H. Tian, J. W. Wu and X. Y. Tian, *Rsc Adv*, 2016, **6**, 5621-5630.
14. R. C. Huber, A. S. Ferreira, R. Thompson, D. Kilbride, N. S. Knutson, L. S. Devi, D. B. Toso, J. R. Challa, Z. H. Zhou, Y. Rubin, B. J. Schwartz and S. H. Tolbert, *Science*, 2015, **348**, 1340-1343.
15. K. A. Iyer and J. M. Torkelson, *Polymer*, 2015, **68**, 147-157.
16. P. Bhagabati, T. K. Chaki and D. Khastgir, *Ind Eng Chem Res*, 2015, **54**, 6698-6712.
17. W. K. Chee, H. N. Lim, N. M. Huang and I. Harrison, *Rsc Adv*, 2015, **5**, 68014-68051.
18. N. Domun, H. Hadavinia, T. Zhang, T. Sainsbury, G. H. Liaghat and S. Vahid, *Nanoscale*, 2015, **7**, 10294-10329.
19. M. F. Zhang, Y. Li, Z. Q. Su and G. Wei, *Polym Chem-Uk*, 2015, **6**, 6107-6124.
20. N. T. Kamar, M. M. Hossain, A. Khomeenko, M. Haq, L. T. Drzal and A. Loos, *Compos Part a-Appl S*, 2015, **70**, 82-92.
21. A. Stojanovic, S. Olveira, M. Fischer and S. Seeger, *Chem Mater*, 2013, **25**, 2787-2792.
22. J. Heo, T. Kang, S. G. Jang, D. S. Hwang, J. M. Spruell, K. L. Killips, J. H. Waite and C. J. Hawker, *J Am Chem Soc*, 2012, **134**, 20139-20145.
23. H. Yang, M. X. Liu, Y. W. Yao, P. Y. Tao, B. P. Lin, P. Keller, X. Q. Zhang, Y. Sun and L. X. Guo, *Macromolecules*, 2013, **46**, 3406-3416.
24. J. Zhao, R. Xu, G. X. Luo, J. Wu and H. S. Xia, *J Mater Chem B*, 2016, **4**, 982-989.
25. D. Wang, Z. B. Zhang, Y. M. Li and C. H. Xu, *Acs Appl Mater Inter*, 2014, **6**, 10014-10021.

26. D. Szmigiel, C. Hibert, A. Bertsch, E. Pamula, K. Domanski, P. Grabiec, P. Prokaryn, A. Scislowska-Czarnecka and B. Plytycz, *Plasma Process Polym*, 2008, **5**, 246-255.
27. U. H. Choi, S. W. Liang, Q. Chen, J. Runt and R. H. Colby, *Acs Appl Mater Inter*, 2016, **8**, 3215-3225.
28. D. F. Schmidt and E. P. Giannelis, *Chem Mater*, 2010, **22**, 167-174.
29. D. P. Dworak and M. D. Soucek, *Macromol Chem Phys*, 2006, **207**, 1220-1232.
30. D. J. Garrett, P. A. Brooksby, F. J. Rawson, K. H. R. Baronian and A. J. Downard, *Anal Chem*, 2011, **83**, 8347-8351.
31. M. Wang, S. M. Sayed, L. X. Guo, B. P. Lin, X. Q. Zhang, Y. Sun and H. Yang, *Macromolecules*, 2016, **49**, 663-671.
32. J. Jiao, X. Sun and T. J. Pinnavaia, *Adv Funct Mater*, 2008, **18**, 1067-1074.
33. Z. J. Wu, Q. Zhuo, T. Sun and Z. Wang, *J Appl Polym Sci*, 2015, **132**, 41409-41414.
34. Y. Ito, W. F. Zhang, J. H. Li, H. X. Chang, P. Liu, T. Fujita, Y. W. Tan, F. Yan and M. W. Chen, *Adv Funct Mater*, 2016, **26**, 1271-1277.
35. R. K. Joshi, P. Carbone, F. C. Wang, V. G. Kravets, Y. Su, I. V. Grigorieva, H. A. Wu, A. K. Geim and R. R. Nair, *Science*, 2014, **343**, 752-754.
36. L. Yu and H. F. Yu, *Acs Appl Mater Inter*, 2015, **7**, 3834-3839.
37. G. M. Viskadourous, M. M. Stylianakis, E. Kymakis and E. Stratakis, *Acs Appl Mater Inter*, 2014, **6**, 388-393.
38. T. Wang, J. H. Huang, Y. Q. Yang, E. Z. Zhang, W. X. Sun and Z. Tong, *Acs Appl Mater Inter*, 2015, **7**, 23423-23430.
39. M. Monti, M. Rallini, D. Puglia, L. Peponi, L. Torre and J. M. Kenny, *Compos Part a-Appl S*, 2013, **46**, 166-172.
40. R. P. Pandey, A. K. Thakur and V. K. Shahi, *Acs Appl Mater Inter*, 2014, **6**, 16993-17002.
41. W. H. Liao, S. Y. Yang, S. T. Hsiao, Y. S. Wang, S. M. Li, C. C. M. Ma, H. W. Tien and S. J. Zeng, *Acs Appl Mater Inter*, 2014, **6**, 15802-15812.
42. M. Naebe, J. Wang, A. Amini, H. Khayyam, N. Hameed, L. H. Li, Y. Chen and B. Fox, *Sci Rep-Uk*, 2014, **4**.
43. A. Guimont, E. Beyou, G. Martin, P. Sonntag and P. Cassagnau, *Macromolecules*, 2011, **44**, 3893-3900.
44. H. W. Kim, H. W. Yoon, S. M. Yoon, B. M. Yoo, B. K. Ahn, Y. H. Cho, H. J. Shin, H. Yang, U. Paik, S. Kwon, J. Y. Choi and H. B. Park, *Science*, 2013, **342**, 91-95.
45. J. Zhong, S. Gao, G. B. Xue and B. Wang, *Macromolecules*, 2015, **48**, 1592-1597.
46. A. R. MacIntosh, K. J. Harris and G. R. Goward, *Chem Mater*, 2016, **28**, 360-367.
47. X. Y. Wang and T. X. Liu, *J Macromol Sci B*, 2011, **50**, 1098-1107.
48. S. Diring, S. Furukawa, Y. Takashima, T. Tsuruoka and S. Kitagawa, *Chem Mater*, 2010, **22**, 4531-4538.
49. Y. S. Bae, A. O. Yazaydin and R. Q. Snurr, *Langmuir*, 2010, **26**, 5475-5483.
50. Z. L. Li, R. J. Young and I. A. Kinloch, *Acs Appl Mater Inter*, 2013, **5**, 456-463.
51. G. Anagnostopoulos, C. Androulidakis, E. N. Koukaras, G. Tsoukleri, I. Polyzos, J. Parthenios, K. Papagelis and C. Galiotis, *Acs Appl Mater Inter*, 2015, **7**, 4216-4223.
52. H. K. Park and K. Y. Park, *Mater Res Bull*, 2008, **43**, 2833-2839.

Graphical Abstract



Schematic representation of the formation process of nanoporous surface of GEOS (left) and the enhanced mechanical performance in PDMS-OH based elastomer (right).

Being compatible with both GEO and polysiloxane, the introduced interfacial layer SiO_2 is nanoporous structure, tunable, and is demonstrated to be an important contributing factor for enhanced stress transmission between GEO and polysiloxane.